DOI: 10.1002/ejoc.200700971

# Stereomutation and Experimental Determination of the Relative Stability of Diastereomeric *O*-Equatorial Anti-Apicophilic Spirophosphoranes

Xin-Dong Jiang,[a] Shiro Matsukawa,[a] Hideaki Yamamichi,[a] Ken-ichiro Kakuda,[a] Satoshi Kojima,[a] and Yohsuke Yamamoto*[a]

**Keywords:** Diastereomers / Hypervalent compounds / Isomerization

A novel bidentate ligand based on 1,1,1,3,3,4,4,4-octafluoro-2-phenyl-2-butanol (**16**) has been used to synthesize a diastereomeric pair of hydrophosphoranes (**18-*exo*** and **18-*endo***). A comparison of the structures of a series of hydrophosphoranes (**18-*exo***, **18-*endo***, **19**, and **20-*exo***) obtained by X-ray crystallography indicated that the apical P–O bond lengths were affected by the electronic properties of the oxygen atom, which can be interpreted by the "single bond/no bond resonance" concept. From the hydrophosphoranes, *O*-apical (**13-*exo*** and **13-*endo***) and anti-apicophilic *O*-equatorial (**12-*exo*** and **12-*endo***) phosphoranes were synthesized. The *O*-equatorial phosphoranes were irreversibly converted into diastereomeric pairs of *O*-apical isomers. Kinetic measurements implied that the electronic properties of the pentafluoroethyl group are comparable to those of the trifluoromethyl group. The activation enthalpies calculated for the stereomutations enabled us for the first time to experimentally show the stability of an *O*-apical isomer to be greater than that of an *O*-equatorial isomer by 13.7 kcal mol$^{-1}$.



## Introduction

Hypervalent[1] 10-P-5[2] phosphorus compounds (phosphoranes) have attracted significant interest and have been widely investigated. Phosphoranes play important roles as intermediates in phosphoryl transfer reactions[3] as well as in synthetic reactions such as the Wittig olefination.[4] Phosphoranes generally adopt trigonal-bipyramidal (TBP) structures that comprise two distinct bonds: the equatorial bond and the apical bond. The apical bond is a weak highly polarizable bond; therefore, electronegative substituents tend to be allocated at the apical rather than the equatorial sites. As for steric factors, it is more favorable for bulky substituents to occupy the less congested equatorial sites. The relative preference of substituents to occupy apical sites is specifically known as apicophilicity.[5,6] In addition, phosphoranes are capable of undergoing stereomutations which are usually explained by the Berry pseudorotation (BPR).[7] BPR is a mechanism involving intramolecular ligand exchange, and this is presumed to be a very low energy process.[8] An alternative mechanism called turnstile rotation (TR) proposed by Ugi et al.[7d,7e] has been calculated to be higher in energy than BPR.[9] Therefore TR is not usually taken into consideration in discussions on the stereomutation of pentacoordinate molecules.

The Martin ligand is known to stabilize the hypervalent state, and a variety of hypervalent compounds of the main group elements have been synthesized (Figure 1).[10] It is particularly worth noting that the Martin ligand, a rigid bidentate ligand, also effectively slows the Berry pseudorotation. We have previously succeeded in isolating phosphoranes having an apical carbon–equatorial oxygen array (**1**: *O*-equatorial) by freezing the BPR, and this happened to be the first example of the isolation of phosphoranes that violate the apicophilicity concept and could still be converted into their more stable stereoisomers (**2**: *O*-apical) (Figure 2).[11–16]

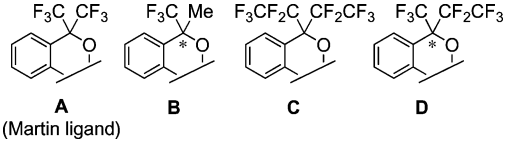


Figure 1. Bidentate ligands.

If we assume that BPR is a valid mechanism for the stereomutation of our spirophosphoranes, consideration of plausible TBP isomers leads to a seven-step process for the conversion between enantiomeric *O*-apical spirophosphoranes, as exemplified by the interconversion of the *n*-butyl-substituted species **2b-*R*$_P$** and **2b-*S*$_P$** (Scheme 1).[17] On this reaction coordinate lie the *O*-equatorial isomers **1b-*R*$_P$** and **1b-*S*$_P$**. Therefore, this latter pair of isomers can be regarded as high-energy intermediates,[11a,11c] and it has been suggested that the overall (global) transition state is common to both the enantiomerization between the *O*-apical

[a] Department of Chemistry, Graduate School of Science, Hiroshima University,
1-3-1 Kagamiyama, Higashi-hiroshima 739-8526, Japan
Fax: +81-82-424-0723
E-mail: yyama@sci.hiroshima-u.ac.jp

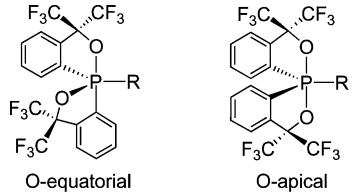


**1a**: R = Me
**1b**: R = *n*Bu
**1c**: R = *t*Bu
**1d**: R = Bn
**3a**: R = NH*n*Pr
**3b**: R = NHBn
**3c**: R = NH*i*Pr
**3d**: R = NH*t*Bu

**2a**: R = Me
**2b**: R = *n*Bu
**2c**: R = *t*Bu
**2d**: R = Bn
**4a**: R = NH*n*Pr
**4b**: R = NHBn
**4c**: R = NH*i*Pr
**4d**: R = NH*t*Bu

Figure 2. Isolated alkylphosphoranes **1** and **2**[11,14] and aminophosphoranes **3** and **4**.[15]

isomers (**2b-$R_P$** and **2b-$S_P$**) and the stereomutation of the *O*-equatorial phosphorane **1b** to the *O*-apical isomer **2b**. Thus, the energy difference in the activation enthalpies for the two processes should provide the difference in the stability of **1b** and **2b** in terms of enthalpy ($\Delta E = \Delta H^{\ddagger}_2 - \Delta H^{\ddagger}_1$). However, the energy of the enantiomerization ($\Delta H^{\ddagger}_2$) was found to be too high to measure by NMR techniques. Thus, we employed a pair of diastereomeric phosphoranes bearing one bidentate ligand **B** (i.e., **5-*exo*** and **5-*endo***) instead. The activation enthalpy for the equilibration of **5** was determined to be 34 kcal mol$^{-1}$, which suggests that $\Delta H^{\ddagger}_2$ for the symmetric system is larger than 34 kcal mol$^{-1}$. Since $\Delta H^{\ddagger}_1$ (**1b** to **2b**) was measured to be 22 kcal mol$^{-1}$, **1b** was determined to be less stable than **2b** by "at least" 12 kcal mol$^{-1}$, as a rather rough estimate.

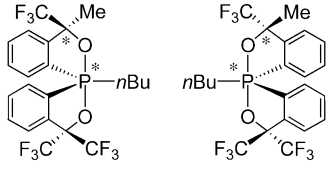

**5-*exo*** **5-*endo***

By using the bidentate ligand **B**, we found a significant stereoelectronic effect on the pseudorotation. The *O*-equatorial diastereomers bearing a *tert*-butyl group as the monodentate ligand (**6-*exo*** and **6-*endo***) exclusively isomerized to the *O*-apical isomers **7-*exo*** and **7-*endo***, respectively (Scheme 2).[18] This stereospecificity could be explained by the difference in the stability of plausible high-energy isomers (**8**–**11**), which could be regarded as having structures similar to those of the actual overall transition states during the multi-step pseudorotation process. Because of the difference in the group electronegativity[19] between the Me and $CF_3$ groups (Me, 2.3; $CF_3$, 3.35),[19a] bidentate ligand **B**, which contains a methyl group, should be less apicophilic than the Martin ligand, making **8** and **11** less stable than **9** and **10**. Conversely, if the methyl group of **6** is replaced by a group R, the selectivity of the stereomutation might give an insight into the relative electronegativity difference between $CF_3$ and R. In any case, as the BPR between stable diastereomers **7** would inevitably go through either high-energy intermediate **8** or **11**, whereas the BPR of **6** to **7** needs to involve only the lower-energy intermediate **9** or **10**. Therefore, this methyl-containing system was not suitable for attempting to determine the experimental stability of the anti-apicophilic *O*-equatorial phosphoranes relative to their stable *O*-apical counterparts.

We recently demonstrated that a bidentate ligand bearing two $C_2F_5$ groups (**C**) is more effective for freezing pseudorotation than the Martin ligand (**A**).[20] Because of the seemingly similar electronegative nature of the $C_2F_5$ group compared with that of $CF_3$, we figured that the use of ligand **D** would decrease the difference in energy among the high-energy isomers corresponding to **8**–**11**, thus permitting us to evaluate the energy difference between *O*-apical and *O*-equatorial isomers. Therefore, we focused on a new bidentate ligand bearing the $C_2F_5$ group (**D**), which is bulkier than a $CF_3$ group, for isolating a complete set of *O*-equatorial and *O*-apical diastereomeric phosphoranes (**12** and **13**) (Figure 3). Although a few studies comparing the group electronegativity of the $C_2F_5$ and $CF_3$ groups have been reported, the order is still contradictory (Lagowski: $CF_3 \geq C_2F_5$,[21a,21b] Tiers: $C_2F_5 > CF_3$,[21c] Zhao: $C_2F_5 > CF_3$[21d]). This disagreement suggests that the electronic properties are rather similar. Thus, as to how the small difference in the electronic nature of the $CF_3$ and $C_2F_5$ groups

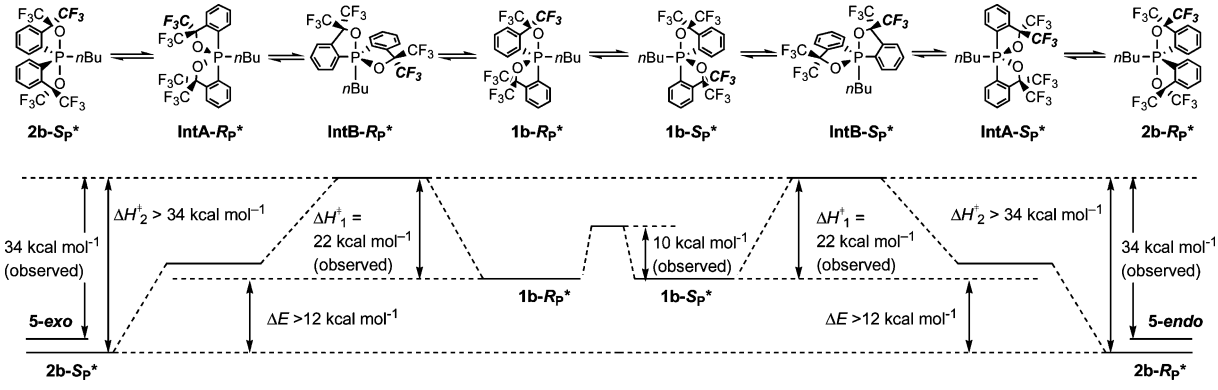


Scheme 1. Energy diagram for the Berry pseudorotation involving **1b**, **2b**, and **5** (***$CF_3$*** denotes the position of the methyl group in **5-*exo*** and **5-*endo***).[11a,11c]

  

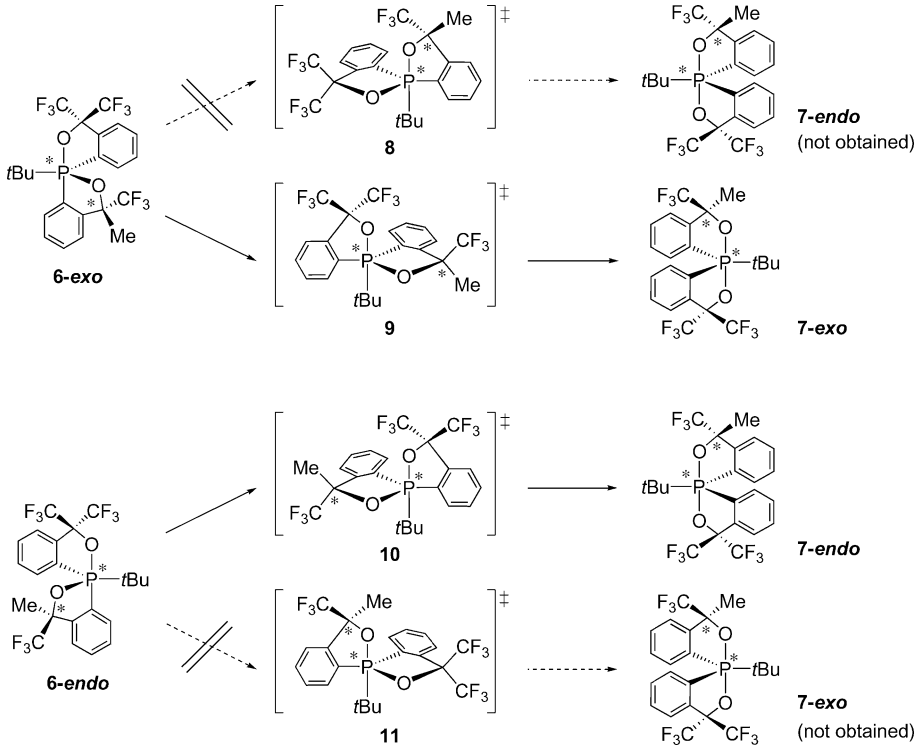


Scheme 2. Stereospecific stereomutation of diastereomeric *O*-equatorial *tert*-butylphosphoranes (**6**).[18]

might affect the selectivity of the stereomutation of **12** to **13** would be of interest.

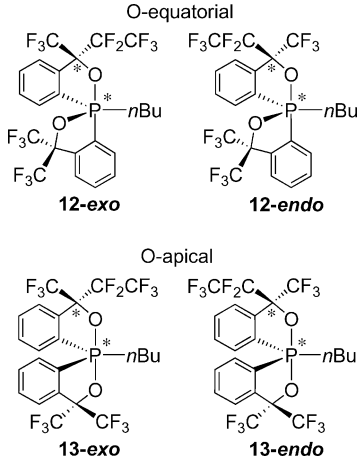


Figure 3. Diastereomeric *O*-equatorial and *O*-apical spirophosphoranes.

We now report the synthesis of a new bidentate ligand **D**, which was used for the synthesis of diastereomeric hydrophosphoranes (**18-*exo*** and **18-*endo***). The *O*-apical phosphoranes **13-*exo*** and **13-*endo*** were diastereoselectively prepared from **18-*exo*** and **18-*endo***, respectively. The *O*-equatorial **12-*exo*** was exclusively prepared from **18-*exo***, whereas **12-*endo*** was prepared from **18-*endo*** as a mixture of **12-*endo*** and **12-*exo*** (92:8). Both *O*-equatorial phosphoranes were found to irreversibly isomerize to the *O*-apical isomers, and the activation energies of the processes were obtained from kinetic measurements. The activation enthalpies of the stereomutation of **12** to **13** suggest that the group electronegativity of the $C_2F_5$ group is comparable to that of the $CF_3$ group. Equilibration between **13-*exo*** and **13-*endo*** was also kinetically measured. This enabled us to experimentally determine the stability of anti-apicophilic *O*-equatorial phosphoranes relative to their stable *O*-apical isomers for the first time. The full details are described in this report.

## Results and Discussion

### Synthesis and Structure of Diastereomeric P–H Spirophosphoranes

1,1,1,3,3,4,4,4-Octafluoro-2-phenyl-2-butanol (**15**)[22] was prepared in 88% yield by the reaction of pentafluoropropiophenone (**14**) with $TMSCF_3$ in the presence of a catalytic amount of tetrabutylammonium fluoride (TBAF) (Scheme 3).[23] Following Martin and co-workers' procedure,[24] compound **15** was dilithiated to furnish **16** by treatment with *n*BuLi in the presence of TMEDA. $Et_2NPCl_2$ was then successively treated with **16** and **17** (dilithiated hexafluorocumyl alcohol)[24] in THF to give a mixture of diastereomeric P–H spirophosphoranes **18** (**18-*exo*/18-*endo*** = 1:2) in 61% yield. The diastereomers of **18** could not be separated by chromatographic techniques on a practical scale. Fortunately, we found that the diastereomeric mixture was subjected to recrystallization from *n*-hexane to give pure **18-*endo*** isomer (24% isolated yield, >98% purity). The filtrate containing **18-*exo*** and **18-*endo*** was then

  

heated at 70 °C to give an equilibrated mixture rich in the **18-*exo*** isomer (**18-*exo*/18-*endo*** = 3.6:1), which recrystallized from acetonitrile to give pure **18-*exo*** (19% isolated yield, >98% purity).

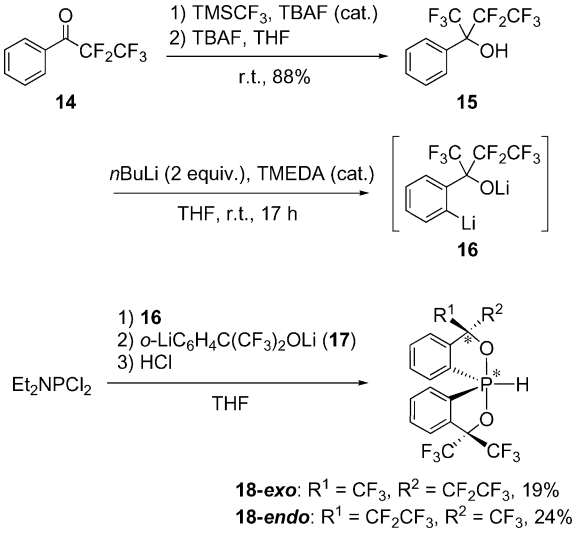


Scheme 3. Synthesis of diastereomeric hydrophosphoranes **18**.

The stereochemistry of each diastereomer was confirmed by X-ray crystallography (Figure 4 and Table 1). The structures of **18-*endo*** and **18-*exo*** are regarded as having a slightly distorted trigonal-bipyramidal (TBP) geometry and are similar to those of the reported compounds **19**[25] and **20-*exo***.[5a] One distinct difference in the structures of **18**–**20** is the apical P–O bond length. Those of **18-*exo***, **18-*endo***, and **19** are in the range of 1.74–1.75 Å. On the other hand, the two P–O bond lengths of **20-*exo*** ($R^2 = CH_3$; P1–O1 = 1.71 Å, P1–O2 = 1.77 Å) are distinctly different. This implies that the P–O lengths are dependent on the electronic nature of the oxygen substituents. This phenomenon can be interpreted by the idea called "single bond/no bond resonance" (Figure 5),[26] that is, if substituent Y is more electronegative than X, the resonance form **A** is more stable than **B**, resulting in the bond length P–Y being longer than that of P–X. Thus, the apparent lower electronegativity of the O1 atom of **20-*exo*** compared with that of the O2 atom

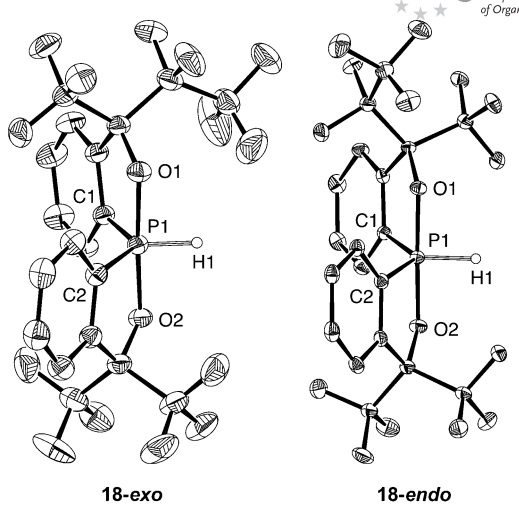


Figure 4. ORTEP diagrams of hydrophosphoranes **18-*exo*** and **18-*endo*** with the thermal ellipsoids at the 30% probability level. All hydrogen atoms other than H1 have been omitted for clarity.

is in good agreement with the bond length of P–O1 being shorter than that of P–O2 by 0.06 Å. Similar findings were reported for some sulfuranes (10-S-4).[27] No noteworthy difference was observed in the P–O bond lengths for **18** and **19**. This is in good agreement with the small difference expected in the group electronegativity between the $CF_3$ and $C_2F_5$ groups.

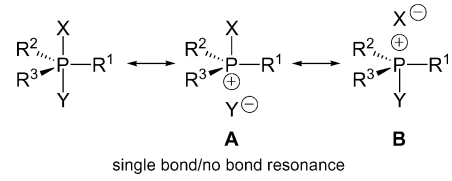


Figure 5. Schematic representation of "single bond/no bond resonance".[26]

The steric bulkiness of the $C_2F_5$ group actually affects the structure of **18**. The two five-membered rings containing the phosphorus atom of **18-*exo*** are nearly planar, whereas those of **18-*endo*** are somewhat distorted probably due to steric repulsion between the *endo*-$C_2F_5$ group and

Table 1. Selected bond lengths and angles for **18-*exo***, **18-*endo***, **19**,[25] and **20**.[5a]


| | **18-*exo*** | **18-*endo*** | **19**[25] | **20-*exo***[5a] |
|---|---|---|---|---|
| Bond lengths [Å] | | | | |
| P1–O1 | 1.7456(16) | 1.750(3) | 1.748(3) | 1.710(2) |
| P1–O2 | 1.7506(16) | 1.749(3) | 1.743(2) | 1.765(2) |
| P1–C1 | 1.805(2) | 1.810(3) | 1.804(4) | 1.814(3) |
| P1–C2 | 1.812(2) | 1.811(4) | 1.809(4) | 1.810(3) |
| Bond angles [°] | | | | |
| O1–P1–O2 | 176.94(8) | 178.40(12) | 178.47(13) | 179.8(1) |
| C1–P1–C2 | 124.82(10) | 125.42(14) | 127.6(2) | 128.7(1) |

  

the *ortho*-proton on the Martin ligand (Figure 6). This is in good agreement with the fact that **18-*exo*** is over three times as stable as **18-*endo*** (see above). Similarly, *O*-apical *n*-butylphosphorane **13-*exo*** is slightly more stable than **13-*endo*** (see below).

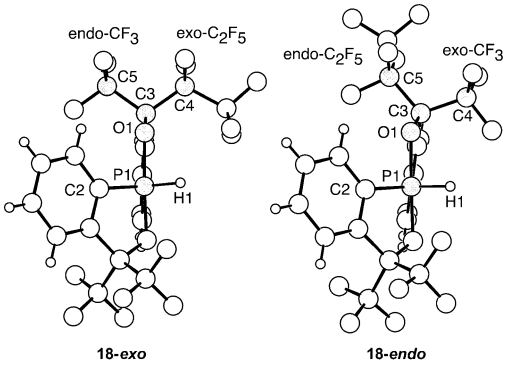


Figure 6. Molecular structures of **18-*exo*** and **18-*endo*** viewed along the P1–C1 bond. Selected dihedral angles [°] for **18-*exo***: P1–O1–C3–C4, –120.78(18); P1–O1–C3–C5, 120.91(18). For **18-*endo***: P1–O1–C3–C4, –102.5(2); P1–O1–C3–C5, 136.2(2).

### Stereospecific Synthesis and Crystal Structures of *O*-Equatorial and *O*-Apical Diastereomeric Spirophosphoranes

*O*-Apical phosphoranes **13** were synthesized by the reaction of **18** with 1-iodobutane in the presence of DBU, with complete retention of stereochemistry (Scheme 4).[28] Following the synthetic method of the *O*-equatorial phosphoranes,[11b,11d] we found that **18-*exo*** almost exclusively produced the *O*-equatorial **12-*exo*** upon treatment with *n*BuLi followed by $I_2$ (Scheme 5 and Table 2). On the other hand, treatment of **18-*endo*** with *n*BuLi produced the *O*-equatorial **12-*endo*** with somewhat lower selectivity (**12-*endo*/12-*exo*** = 92:8). All the *O*-equatorial phosphoranes irreversibly converted into the *O*-apical isomers when heated in solution (see below).

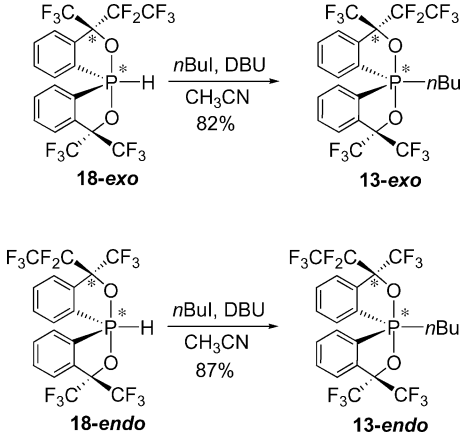


Scheme 4. Synthesis of *O*-apical spirophosphoranes **13**.

As symmetric *O*-equatorial spirophosphoranes are known to undergo rapid interconversion between enantiomers by a one-step pseudorotation with the monodentate ligand as a pivot,[11a,11c,29] we expected to see the presence of two species. For the *O*-equatorial **12-*exo***, the single signal ($\delta$ = –2.6 ppm) observed in the $^{31}$P NMR spectrum at room temperature in [$D_8$]toluene decoalesced into two signals (major: $\delta$ = –2.3 ppm; minor: $\delta$ = –2.8 ppm) at –80 °C. In the $^{19}$F NMR spectrum, the four $CF_3$ signals observed in [$D_8$]toluene at room temperature ($\delta$ = –73.8, –74.3, –75.6, and –79.3 ppm) decoalesced into eight signals at low temperatures (major: $\delta$ = –73.1, –73.5, –75.3, and –78.9 ppm; minor: $\delta$ = –73.7, –73.8, –74.7, and –78.6 ppm at –80 °C), as shown in Figure 7. For the latter two signals (–75.6 and –79.3 ppm), the decoalescence temperatures ($T_c$) were –36 and –44 °C, respectively. Therefore, the activation free energy could be roughly estimated to be 11 kcal mol$^{-1}$ at these temperatures. These two sets of $^{31}$P and $^{19}$F NMR signals could be considered to correspond to **12-*exo*-A** and **12-*exo*-B**, respectively, as shown in Scheme 6. The major/minor ratio is 3.5:1 at –80 °C ($\Delta G°_{193}$ = 0.48 kcal mol$^{-1}$). It is not clear which isomer is the more stable.

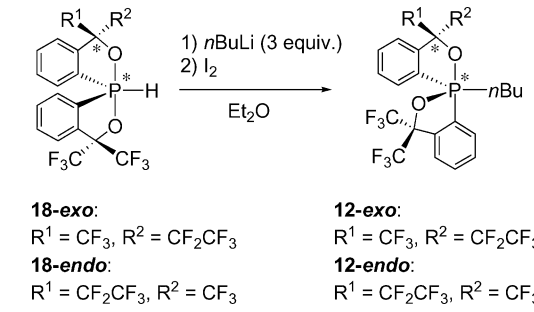


Scheme 5. Synthesis of *O*-equatorial spirophosphoranes **12**.

Table 2. Yield and ratio of **12-*exo*** and **12-*endo***.

| **18** | % Yield | **12-*exo*/12-*endo*** |
|---|---|---|
| **18-*exo*** | 87 | >99:1 |
| **18-*endo*** | 77 | 8:92 |

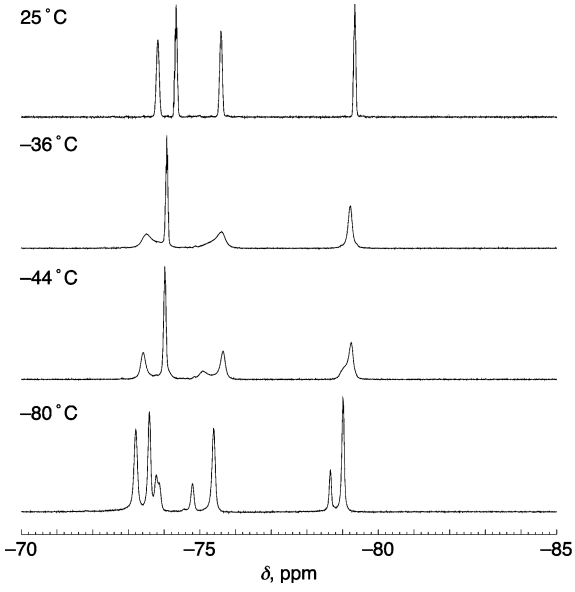


Figure 7. Variable-temperature $^{19}$F NMR spectra of **12-*exo***.

  

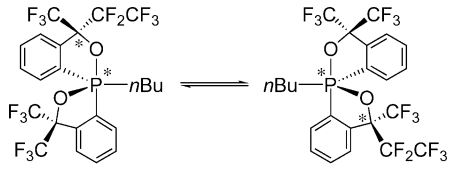


Scheme 6. One-step pseudorotation between *O*-equatorial diastereomers.

The stereochemistries of the *n*-butylphosphoranes **12-*exo*** and **13-*exo*** were determined by X-ray analysis (Figure 8 and Table 3). For the *O*-equatorial isomer, **12-*exo*-A** was observed in which the bidentate ligand, including the pentafluoroethyl group, was found to adopt the *O*-apical *C*-equatorial configuration.

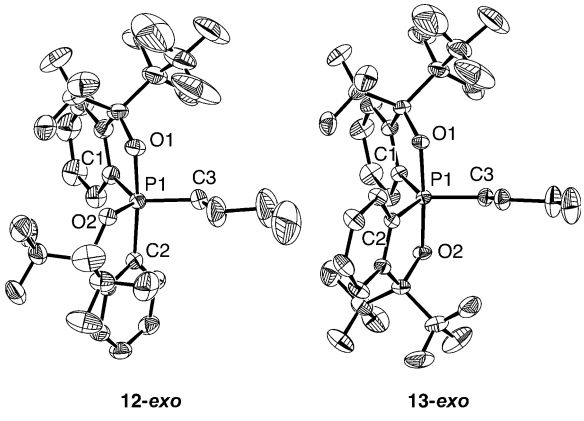


Figure 8. ORTEP diagrams of **12-*exo*** and **13-*exo*** with the thermal ellipsoids at the 30% probability level. All the hydrogen atoms have been omitted for clarity.

Table 3. Selected bond lengths and angles for **12-*exo*** and **13-*exo***.

| | **12-*exo*** | **13-*exo*** |
|---|---|---|
| Bond lengths [Å] | | |
| P1–O1 | 1.7798(19) | 1.762(2) |
| P1–O2 | 1.6636(17) | 1.759(2) |
| P1–C1 | 1.822(2) | 1.820(3) |
| P1–C2 | 1.870(2) | 1.821(3) |
| P1–C3 | 1.827(3) | 1.822(3) |
| Bond angles [°] | | |
| O1–P1–O2 | 82.61(9) | 175.68(12) |
| O1–P1–C1 | 87.31(11) | 87.09(12) |
| O1–P1–C2 | 170.24(10) | 90.90(12) |
| O1–P1–C3 | 89.53(13) | 91.37(14) |
| O2–P1–C1 | 120.88(10) | 90.99(12) |
| O2–P1–C2 | 87.64(9) | 87.08(12) |
| O2–P1–C3 | 119.31(13) | 92.95(14) |
| C1–P1–C2 | 97.39(11) | 125.82(14) |
| C1–P1–C3 | 118.67(14) | 117.17(15) |
| C2–P1–C3 | 95.64(13) | 117.01(14) |

## Possible Mechanism for the Diastereospecific Formation of the *O*-Equatorial Phosphoranes

A plossible mechanism for the formation of **12-*exo*** is shown in Scheme 7. Nucleophilic attack on a TBP molecule can be regarded as occurring within the equatorial plane.[14,30] As there are two $\sigma^*_{P-C}$ orbitals in the plane, there are two possible pathways (**a** and **b**) for the attack of *n*BuLi on phosphorane-ide **21-*exo*** generated from **18-*exo***. We have demonstrated that the *O*-equatorial phosphorane

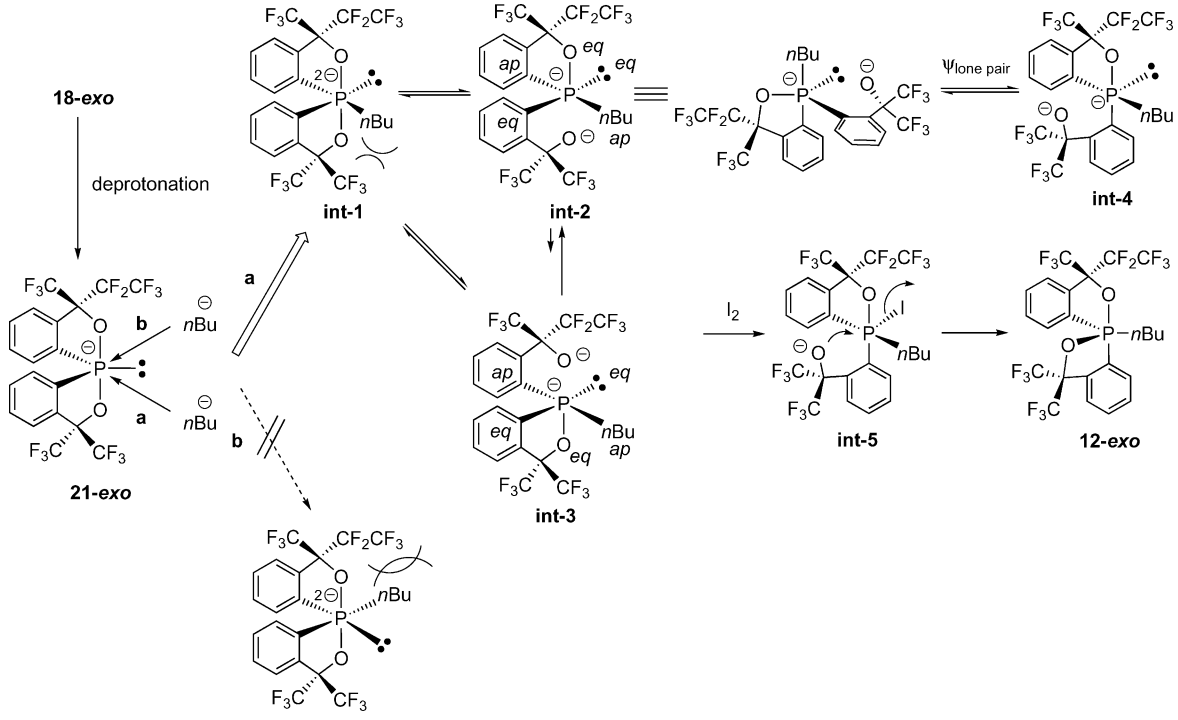


Scheme 7. Proposed mechanism for the diastereospecific formation of **12-*exo*** from **18-*exo***.

  

bearing two Martin ligands (**1b**) readily reacted with MeLi to give compound **22**,[14] whereas compound **23**, which has four pentafluoroethyl groups, did not react at all (Scheme 8).[31] This indicated that the nucleophilic attack upon **23** was prevented by the steric bulk of the $C_2F_5$ groups. Thus, it could be assumed that path **a** is preferred. The crystal structure of the hydrophosphorane **18-*exo*** (Figure 6) supports this notion. Attack by path **a** provides a dianion (**int-1**) in which there are two P–O bonds that can be cleaved. The lower P–O bond should be preferentially cleaved because of the steric repulsion between *n*Bu and the $CF_3$ group. In addition, the resulting pentacoordinate intermediate **int-2** should be more stable than **int-3** because either the bidentate Martin ligand of **int-3** would span two equatorial positions or a lone pair would occupy an apical site in a trigonal-pyramidal arrangement. The intermediate **int-2** can then undergo BPR to form the more stable isomeric **int-4**. The attack of $I_2$ on **int-4** would be sterically favorable with the *ortho* substituent of the monodentate Martin ligand rotated in between the bidentate P–C bond and the *n*Bu group and away from the lone pair. Thus, upon formation of the iodide (**int-5**) by attack of $I_2$, the oxide anion is positioned to make a concomitant intramolecular attack on the opposite side of the iodide to furnish the *O*-equatorial **12-*exo***, as observed.

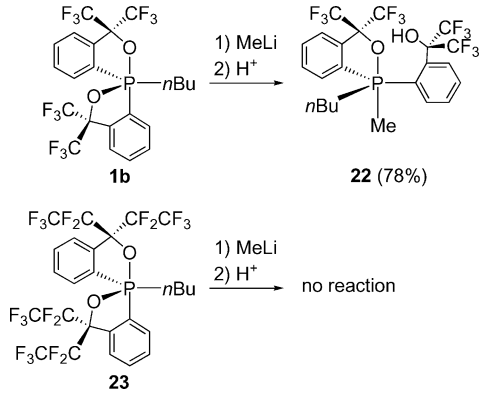


Scheme 8. Steric effect of the pentafluoroethyl group during the reaction with MeLi.[14,31]

The diastereoselectivity in the formation of **12-*endo*** was also very high but a bit lower than that of **12-*exo*** (Scheme 5 and Table 2). This can also be explained in terms of the steric repulsion of the pentafluoroethyl group. As the X-ray structure of **18-*endo*** shows, a "buttressing effect"[32] caused by the steric repulsion between the *endo*-$C_2F_5$ group and the aromatic ring of the Martin ligand forces the ring bearing the $C_2F_5$ group to tilt towards the equatorial hydrogen atom. The same situation is expected for **21-*endo***, resulting

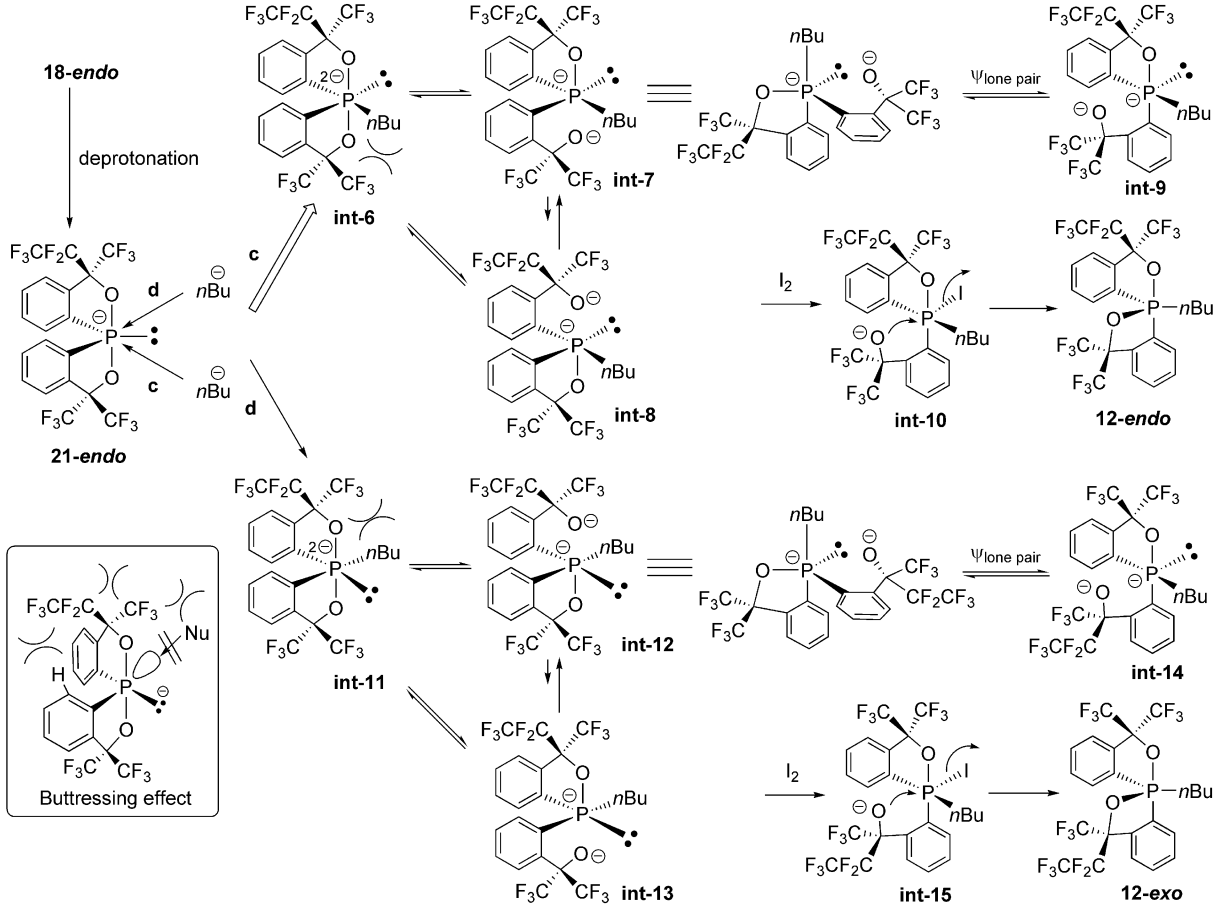


Scheme 9. Proposed mechanism for the diastereospecific formation of **12-*endo***.

  

in steric hindrance in the vicinity of this bidentate ligand (Figure 6). Therefore, attack by path **c** is assumed to be preferred to path **d**, as shown in Scheme 9.

## Kinetic Study

### *Stereomutation between 13-exo and 13-endo*

The *O*-apical phosphorane **13-*exo*** was heated at 190 °C in 4-*tert*-butyltoluene for 6 h to give an equilibrated mixture of **13-*exo*** and **13-*endo*** (1.9:1.0) (Scheme 10). Kinetic measurements of the reversible isomerization between **13-*exo*** and **13-*endo*** were carried out in 4-*tert*-butyltoluene over the temperature range of 190–210 °C by monitoring the change in the $^{19}F$ NMR integrals of the $CF_3$ groups. The measurements obeyed reversible first-order kinetics. The activation parameters were obtained by using the Eyring plot (Figure 9) and the data are shown in Table 4. The averaged activation enthalpy for the stereomutation of **13** is 36.3 kcal mol$^{-1}$, and this is greater than that for *C*-methyl-substituted **5** (33.7 kcal mol$^{-1}$) by 2.6 kcal mol$^{-1}$.

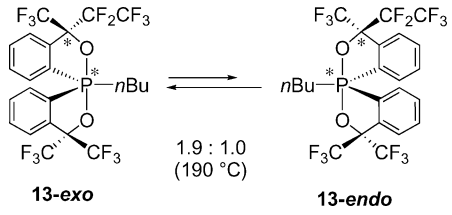


Scheme 10. Stereomutation between **13-*exo*** and **13-*endo*** in 4-*tert*-butyltoluene.

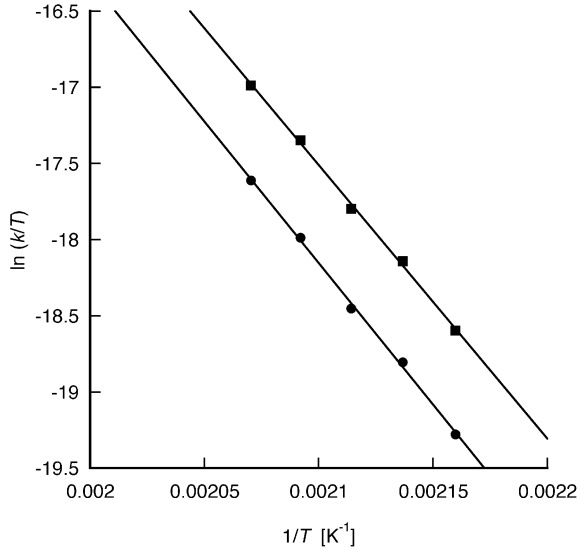


Figure 9. Eyring plot for the stereomutation between **13-*exo*** and **13-*endo***. Square: **13-*exo*** to **13-*endo***; circle: **13-*endo*** to **13-*exo***.

### *Stereomutation of 12 to 13*

A solution of **12-*exo*** in 4-*tert*-butyltoluene was heated at 60 °C for 8 h to give a mixture of the *O*-apical **13-*exo*** and **13-*endo*** (**13-*exo*/13-*endo*** = 1.0:2.2). On the other hand, upon heating **12-*endo*** under similar conditions, a mixture of the *O*-apical phosphoranes with a different ratio (**13-*exo*/13-*endo*** = 6.9:1.0) was obtained (Scheme 11). Kinetic measurements of the stereomutation of **12** to **13** were carried out in 4-*tert*-butyltoluene at 40–60 °C by monitoring the change in the $^{19}F$ NMR integrals of the $CF_3$ groups. The activation parameters were obtained as before by using the Eyring plot (Figure 10) and the data are shown in Table 5. The activation enthalpies for all four processes are essentially the same (avg. 22.6 kcal mol$^{-1}$) and slightly greater than that for **1b** to **2b** (21.8 kcal mol$^{-1}$). The difference in

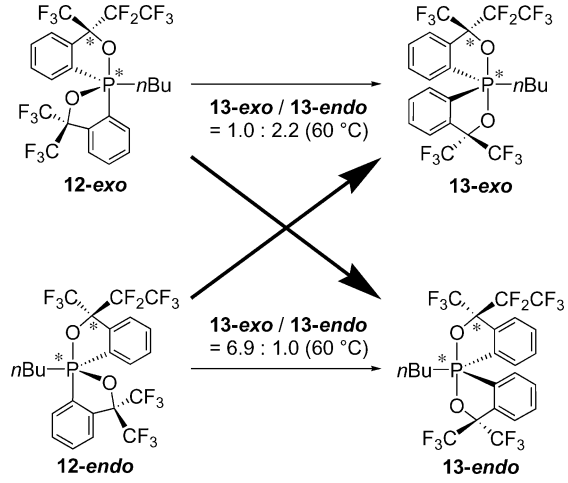


Scheme 11. Stereomutation of *O*-equatorial **12** to *O*-apical **13** in 4-*tert*-butyltoluene.

Table 4. Rate constants and activation parameters for the stereomutation between **13-*exo*** and **13-*endo***.[a]

| Process | *T* [K] | Equilibrium ratio **13-*exo*/13-*endo*** | *k* [s$^{-1}$] | $\Delta H^{\ddagger}$ [kcal mol$^{-1}$] | $\Delta S^{\ddagger}$ [e.u.] | $\Delta G^{\ddagger}_{333}$ [kcal mol$^{-1}$] |
|---|---|---|---|---|---|---|
| | 463 | 1.98:1.00 | $(1.96 \pm 0.02) \times 10^{-6}$ | | | |
| | 468 | 1.94:1.00 | $(3.19 \pm 0.06) \times 10^{-6}$ | | | |
| **13-*exo*** to **13-*endo*** | 473 | 1.92:1.00 | $(4.58 \pm 0.06) \times 10^{-6}$ | 36.9 ± 0.9 | –5.8 ± 1.8 | 38.8 |
| | 478 | 1.90:1.00 | $(7.37 \pm 0.17) \times 10^{-6}$ | | | |
| | 483 | 1.87:1.00 | $(1.08 \pm 0.02) \times 10^{-5}$ | | | |
| | 463 | 1.98:1.00 | $(3.88 \pm 0.03) \times 10^{-6}$ | | | |
| | 468 | 1.94:1.00 | $(6.18 \pm 0.11) \times 10^{-6}$ | | | |
| **13-*endo*** to **13-*exo*** | 473 | 1.92:1.00 | $(8.81 \pm 0.12) \times 10^{-6}$ | 35.7 ± 0.8 | –7.1 ± 1.7 | 38.0 |
| | 478 | 1.90:1.00 | $(1.40 \pm 0.03) \times 10^{-5}$ | | | |
| | 483 | 1.87:1.00 | $(2.02 \pm 0.05) \times 10^{-5}$ | | | |

[a] Error is denoted as standard deviation.

  

Table 5. Rate constants and activation parameters for the stereomutation of **12** to **13**.[a]

| Process | $T$ [K] | $k$ [$s^{-1}$] | $\Delta H^{\ddagger}$ [kcal mol$^{-1}$] | $\Delta S^{\ddagger}$ [e.u.] | $\Delta G^{\ddagger}_{333}$ [kcal mol$^{-1}$] |
|---|---|---|---|---|---|
| | 313 | $(8.99 \pm 0.33) \times 10^{-6}$ | | | |
| | 318 | $(1.55 \pm 0.05) \times 10^{-5}$ | | | |
| **12-*exo*** to **13-*exo*** | 323 | $(2.83 \pm 0.04) \times 10^{-5}$ | 22.7 ± 0.3 | –9.0 ± 1.0 | 25.6 |
| | 328 | $(5.08 \pm 0.06) \times 10^{-5}$ | | | |
| | 333 | $(8.38 \pm 0.09) \times 10^{-5}$ | | | |
| | 313 | $(2.01 \pm 0.03) \times 10^{-5}$ | | | |
| | 318 | $(3.51 \pm 0.05) \times 10^{-5}$ | | | |
| **12-*exo*** to **13-*endo*** | 323 | $(6.32 \pm 0.04) \times 10^{-5}$ | 22.7 ± 0.2 | –7.6 ± 0.8 | 25.2 |
| | 328 | $(1.13 \pm 0.01) \times 10^{-4}$ | | | |
| | 333 | $(1.88 \pm 0.01) \times 10^{-4}$ | | | |
| | 313 | $(3.41 \pm 0.03) \times 10^{-5}$ | | | |
| | 318 | $(6.13 \pm 0.05) \times 10^{-5}$ | | | |
| **12-*endo*** to **13-*exo*** | 323 | $(1.07 \pm 0.01) \times 10^{-4}$ | 22.6 ± 0.2 | –6.6 ± 0.7 | 24.9 |
| | 328 | $(1.85 \pm 0.01) \times 10^{-4}$ | | | |
| | 333 | $(3.28 \pm 0.02) \times 10^{-4}$ | | | |
| | 313 | $(5.19 \pm 0.26) \times 10^{-6}$ | | | |
| | 318 | $(9.20 \pm 0.47) \times 10^{-6}$ | | | |
| **12-*endo*** to **13-*endo*** | 323 | $(1.57 \pm 0.04) \times 10^{-5}$ | 22.4± 0.3 | –11.1 ± 0.8 | 26.1 |
| | 328 | $(2.85 \pm 0.06) \times 10^{-5}$ | | | |
| | 333 | $(4.78 \pm 0.17) \times 10^{-5}$ | | | |

[a] Error is denoted as standard deviation.

$\Delta G^{\ddagger}$ [25.6 (**12-*exo*** to **13-*exo***), 25.2 (**12-*exo*** to **13-*endo***), 24.9 (**12-*endo*** to **13-*exo***), and 26.1 (**12-*endo*** to **13-*endo***) kcal mol$^{-1}$] mainly comes from the difference in $\Delta S^{\ddagger}$, which is probably related to the steric bulk of the $C_2F_5$ group.

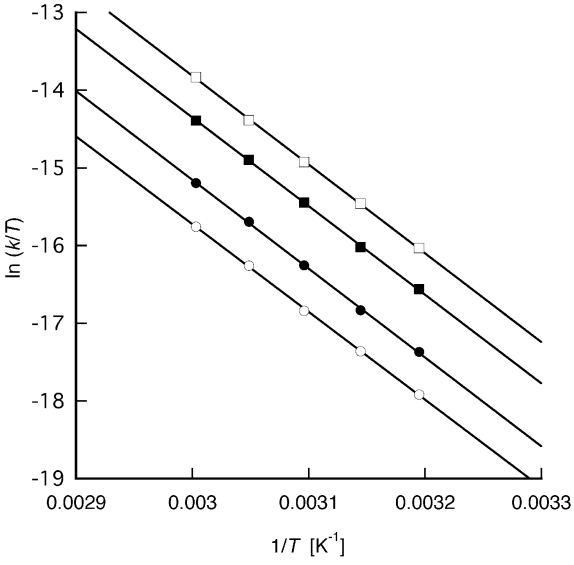


Figure 10. Eyring plot for the stereomutation of **12** to **13**. Open circles: **12-*endo*** to **13-*endo***; open squares: **12-*endo*** to **13-*exo***; filled circles: **12-*exo*** to **13-*exo***; filled squares: **12-*exo*** to **13-*endo***.

### *Relative Stability of O-Equatorial and O-Apical Spirophosphoranes*

The stereomutation pathways for the system involving **12** and **13** can be depicted by the Desargus–Levi diagram[7b] in which the structurally disallowed stereoisomers (*13*, *31*, *24*, and *42*) have been removed (Figure 11). As previously discussed,[5a] isomers *35*, *53*, *45*, and *54* are considered to be the least favorable as intermediates because not only does one of the bidentate ligands span two equatorial sites to induce ring strain but also because the two oxygen atoms occupy equatorial sites. Therefore, routes involving these isomers can be eliminated from the possible stereomutation pathways. According to this diagram, there are two conceivable low-energy pathways for the equilibration between **13-*exo*** and **13-*endo***.

As the *O*-apical isomer **13-*exo*** was found to be only slightly more stable than **13-*endo*** (Scheme 9), it would be rational to assume that the difference in stability between *O*-equatorial **12-*endo*** and **12-*exo*** is also very small, thereby slightly favoring the latter. Therefore, it is no surprise that the stereomutation between **13-*exo*** and **13-*endo*** took place by both routes (the *exo* and *endo* path in Figure 11). As the activation enthalpies ($\Delta H^{\ddagger}$) of the stereomutation of **12** to **13** are essentially the same (avg. 22.6 kcal mol$^{-1}$), we deduced that the *O*-equatorial phosphorane **12** is less stable than the *O*-apical counterpart **13** by 13.7 (36.3–22.6) kcal mol$^{-1}$ based on the activation enthalpies of this system (Figure 12). This provides the first direct experimental evaluation of the stability of an anti-apicophilic phosphorane relative to its more stable *O*-apical isomer. The value of 13.7 kcal mol$^{-1}$ is in good agreement with the calculated difference between *O*-equatorial phosphorane **1a** and *O*-apical phosphorane **2a** of 14.1 kcal mol$^{-1}$.[14] This conformity, in turn, supports the validity of the BPR mechanism for the stereomutation of phosphoranes, on which mechanism we have based our considerations. Based on the very similar $\Delta H^{\ddagger}$ values, we can regard the thermodynamic stabilities of the assumed high-energy isomers (*15*, *51*, *25*, and *52*) as being almost the same. In terms of electronic effects, this implies that the group electronegativities of $CF_3$ and $C_2F_5$ are comparable.

  

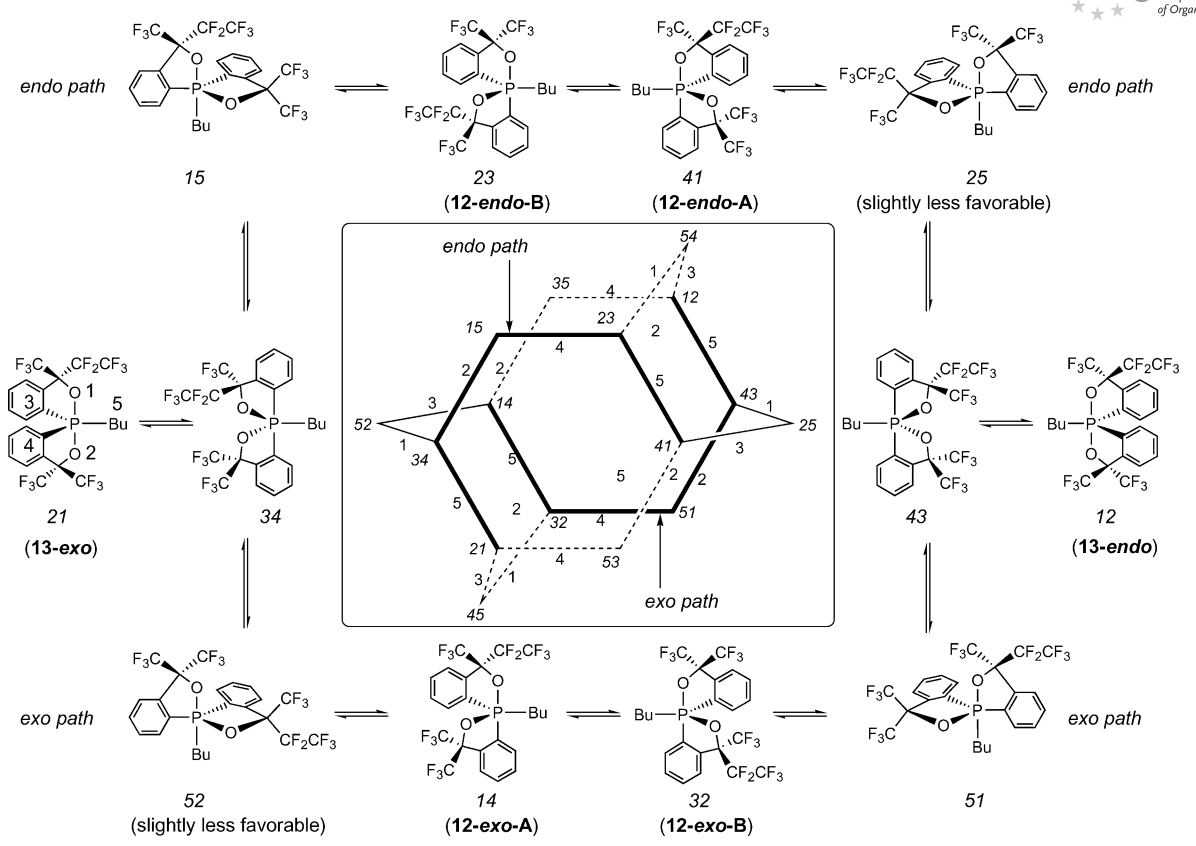


Figure 11. Restricted Desargus–Levi diagram. The double digits correspond to diastereomers and the single digits to the pivot substituent of the pseudorotation process.

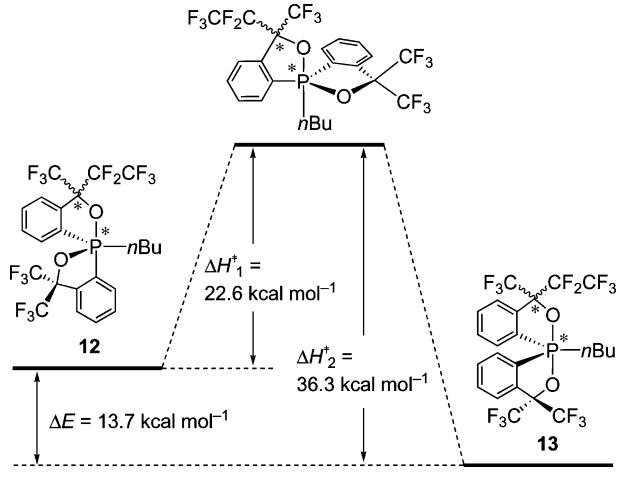


Figure 12. The relative stability of *O*-equatorial **12** and *O*-apical **13**.

## Conclusions

A bidentate ligand bearing a $CF_3$ and a $C_2F_5$ group has been synthesized and used for the synthesis of a diastereomeric pair of hydrophosphoranes (**18-*exo*** and **18-*endo***). The diastereomer **18-*endo*** could be isolated by simply recrystallizing from *n*-hexane, whereas **18-*exo*** could be obtained by recrystallization from acetonitrile after increasing its diastereomeric ratio by heating in solution. The crystal structures of **18-*exo*** and **18-*endo*** were confirmed by single-crystal X-ray analysis. In **18-*endo***, the five-membered rings were found to be slightly distorted due to steric repulsion originating from the *endo*-$C_2F_5$ group. A comparison of the structures of **18**, **19**, and **20-*exo*** revealed that the apical P–O bond lengths of **18** and **19** are comparable (1.74–1.75 Å), whereas in **20-*exo***, the P–O1 distance (1.71 Å) was found to be shorter than that of P–O2 (1.77 Å). This result can be explained by the "single bond/no bond resonance" concept. The *O*-apical *n*-butylphosphoranes (**13-*exo*** and **13-*endo***) were prepared from the hydrophosphoranes **18-*exo*** and **18-*endo***, respectively, with retention of stereochemistry. Kinetic measurements of the equilibration between **13-*exo*** and **13-*endo*** suggest that the former is slightly more stable than the latter. The *O*-equatorial *n*-butylphosphorane **12-*exo*** was synthesized as the exclusive product from **18-*exo***, whereas the selectivity in the synthesis of **12-*endo*** (*endo*/*exo* = 92:8) was somewhat lower than that of **12-*exo***. The *O*-equatorial phosphoranes irreversibly isomerized into diastereomeric mixtures of *O*-apical phosphoranes with low selectivities [**13-*exo*/13-*endo*** = 1.0:2.2 (from **12-*exo***) and 6.9:1.0 (from **12-*endo***)]. However, this in turn enabled us to experimentally determine the stability of the *O*-equatorial isomer **12** relative to the *O*-apical phosphorane **13**. For the *O*-equatorial isomers **12**, the activation enthalpies for their irreversible stereomutation to **13**

  

are essentially the same for all four processes. Based on a comparison of the activation enthalpies, the *O*-apical phosphorane **13** was found to be more stable than the *O*-equatorial isomer **12** by 13.7 kcal mol$^{-1}$. The results presented here are yet another step towards gaining a full picture of the complex BPR mechanism.

## Experimental Section

**General:** The melting points were measured with a Yanaco micro-melting point apparatus. The $^1$H (400 MHz), $^{19}$F (376 MHz), and $^{31}$P NMR (162 MHz) spectra were recorded with a JEOL EX-400 or AL-400 spectrometer. The $^1$H NMR chemical shifts ($\delta$) are given in ppm downfield from $Me_4Si$, determined by residual chloroform ($\delta$ = 7.26 ppm). The $^{19}$F NMR chemical shifts ($\delta$) are given in ppm downfield from external $CFCl_3$. The $^{31}$P NMR chemical shifts ($\delta$) are given in ppm downfield from external 85% $H_3PO_4$. The elemental analyses were performed with a Perkin-Elmer 2400 CHN elemental analyzer. All reactions were carried out under $N_2$. Tetrahydrofuran (THF) and diethyl ether ($Et_2O$) were freshly distilled from Na/benzophenone, *n*-hexane was distilled from Na, and the other solvents were distilled from $CaH_2$. Merck silica gel 60 was used for column chromatography.

**1,1,1,3,3,4,4,4-Octafluoro-2-phenyl-2-butanol (15):**[22] Under $N_2$, TBAF (1.0 M solution in THF, 0.19 mL, 0.19 mmol) was added to a mixture of $TMSCF_3$ (7.8 mL, 49 mmol) and **14** (10.4 g, 46.6 mmol) at 0 °C. The mixture was stirred for 3 h at room temperature. In the open air, THF (unpurified, 15 mL) and TBAF (1.0 M solution in THF, 3.0 mL, 3.0 mmol) was added to the mixture, then the mixture was stirred for 20 h at room temperature. The reaction was quenched with 2 M HCl (100 mL). The mixture was extracted with $Et_2O$ (150 mL × 2), then the organic layer was washed with brine (100 mL × 2) and dried with anhydrous $MgSO_4$. After removing the solvents by evaporation, the resulting yellow oil was distilled to afford a colorless liquid of **15** (12.1 g, 41.3 mmol, 88%); b.p. 71–72 °C/25 Torr (ref.[22] 66–68 °C/20 mbar). $^1$H NMR ($CDCl_3$): $\delta$ = 7.72 (d, $^3J_{H,H}$ = 7.2 Hz, 2 H), 7.48–7.42 (m, 3 H), 3.65 (s, 1 H) ppm. $^{19}$F NMR ($CDCl_3$): $\delta$ = –74.3 (dd, $^3J_{F-F}$ = 12.4, $^3J_{F-F}$ = 11.2 Hz, 3 F), –78.7 (s, 3 F), –120.3 (dq, $^2J_{F-F}$ = 284.6, $^3J_{F-F}$ = 11.2 Hz, 1 F), –122.1 (dq, $^2J_{F-F}$ = 284.6, $^3J_{F-F}$ = 12.4 Hz, 1 F) ppm.

**18-*exo* and 18-*endo*:** Under $N_2$, TMEDA (0.20 mL, 1.3 mmol) was added to *n*BuLi (1.60 M *n*-hexane solution, 1.7 mL, 2.7 mmol) at room temperature and the mixture was stirred for 15 min. Alcohol **15** (0.396 g, 1.34 mmol) in THF (0.1 mL) was then added to the mixture at 0 °C and stirring was continued for 17 h at room temperature. The mixture was added to a solution of $Et_2NPCl_2$ (0.19 mL, 1.3 mmol) in THF (1 mL) at –78 °C and the resulting mixture was stirred for 7 h at room temperature. At –78 °C, lithium 1,1,1,3,3,3-hexafluoro-2-(2-lithiophenyl)-2-propoxide (**17**), prepared from the reaction of 1,1,1,3,3,3-hexafluoro-2-phenyl-2-propanol (0.25 mL, 1.5 mmol) with *n*BuLi (1.60 M *n*-hexane solution, 1.8 mL, 2.9 mmol) in the presence of TMEDA (0.20 mL, 1.3 mmol), was added to the mixture. The resulting mixture was stirred for 10 h at room temperature. The reaction was quenched with 6 M HCl (50 mL) at 0 °C. The mixture was extracted with $Et_2O$ (50 mL × 2), then the organic layer was washed with brine (40 mL × 2), and dried with anhydrous $MgSO_4$. After removing the solvents by evaporation, the resulting crude mixture was separated by column chromatography ($CH_2Cl_2$/*n*-hexane = 1:5) to afford **18** as a white solid (452 mg, 0.799 mmol, 62%, **18-*exo*/18-*endo*** = 1:2). The mixture was subjected to recrystallization (*n*-hexane) to afford colorless crystals of **18-*endo*** (177 mg, 0.313 mmol, 24%). Afterwards the filtrate was evaporated, the residue was dissolved in $CHCl_3$ (10 mL), and then heated at 70 °C for 8 h. After removing the solvents by evaporation, an **18-*exo*-**enriched mixture (**18-*exo*/18-*endo*** = 3.6:1) was obtained. The mixture was subjected to recrystallization (MeCN) to afford colorless crystals of **18-*exo*** (143 mg, 0.253 mmol, 19%). Colorless crystals of **18-*endo*** and **18-*exo*** suitable for X-ray analysis were obtained by further recrystallization from *n*-hexane/$Et_2O$ and MeCN, respectively. **18-*endo***: $^1$H NMR ($CDCl_3$): $\delta$ = 8.34–8.28 (m, 2 H), 8.26 (d, $^1J_{H-P}$ = 726.8 Hz, 1 H), 7.82–7.71 (m, 6 H) ppm. $^{19}$F NMR ($CDCl_3$): $\delta$ = –74.5 (tq, $^3J_{F-F}$ = 9.9, $^5J_{F-F}$ = 4.9 Hz, 3 F), –75.1 (q, $^4J_{F-F}$ = 9.8 Hz, 3 F), –76.2 (q, $^4J_{F-F}$ = 9.8 Hz, 3 F), –79.1 (q, $^5J_{F-F}$ = 4.9 Hz, 3 F), –119.1 (q, $^3J_{F-F}$ = 9.9 Hz, 2 F) ppm. $^{31}$P NMR ($CDCl_3$): $\delta$ = –45.8 ppm. M.p. 102.2–103.0 °C (dec.). $C_{19}H_9F_{14}O_2P$ (566.22): calcd. C 40.30, H 1.60; found C 39.97, H 1.90. **18-*exo***: $^1$H NMR ($CDCl_3$): $\delta$ = 8.33–8.26 (m, 2 H), 8.28 (d, $^1J_{H-P}$ = 736.4 Hz, 1 H), 7.78–7.71 (m, 6 H) ppm. $^{19}$F NMR ($CDCl_3$): $\delta$ = –73.5 (dq, $^3J_{F-F}$ = 12.3, $^5J_{F-F}$ = 4.9 Hz, 3 F), –75.0 (q, $^4J_{F-F}$ = 8.6 Hz, 3 F), –76.2 (q, $^4J_{F-F}$ = 8.6 Hz, 3 F), –79.1 (dq, $^4J_{F-F}$ = 8.6, $^5J_{F-F}$ = 4.9 Hz, 3 F), –116.5 (dq, $^2J_{F-F}$ = 288.3, $^4J_{F-F}$ = 8.6 Hz, 1 F), –120.5 (dq, $^2J_{F-F}$ = 288.3, $^3J_{F-F}$ = 12.3 Hz, 1 F) ppm. $^{31}$P NMR ($CDCl_3$): $\delta$ = –45.3 ppm. M.p. 122.5–123.1 °C. $C_{19}H_9F_{14}O_2P$ (566.22): calcd. C 40.30, H 1.60; found C 40.03, H 1.29.

**Phosphorane 12:** Under $N_2$, *n*BuLi (1.60 M *n*-hexane solution, 0.15 mL, 0.24 mmol) was added to a solution of **18** (45.3 mg, 0.080 mmol, **18-*exo*/18-*endo*** = 1:1) in $Et_2O$ (3 mL) at 0 °C and the mixture was stirred for 3 h at room temperature. $I_2$ (61 mg, 0.24 mmol) was then added to the mixture at –78 °C and stirring was continued for 3 h at room temperature. The reaction was quenched with aqueous $Na_2S_2O_3$ (50 mL). The mixture was extracted with $Et_2O$ (60 mL × 2), and the organic layer was washed with brine (50 mL × 2) and dried with anhydrous $MgSO_4$. After removing the solvents by evaporation, the resulting crude mixture was separated by preparative TLC ($Et_2O$/*n*-hexane = 1:5) to afford a mixture of **12** (40.9 mg, 0.065 mmol, 82%, **12-*exo*/12-*endo*** = 1:1). The mixture was separated by reversed-phase HPLC ($CH_3CN$) to afford **12-*exo*** ($t_R$ = 26.4 min, 13.7 mg, 0.022 mmol, 28%) and **12-*endo*** ($t_R$ = 27.2 min, 19.4 mg, 0.031 mmol, 39%) as white solids. Colorless crystals of **12-*exo*** suitable for X-ray analysis were obtained by recrystallization from *n*-hexane. **12-*exo***: $^1$H NMR ($CDCl_3$): $\delta$ = 7.77–7.71 (m, 2 H), 7.65–7.54 (m, 6 H), 2.52–2.42 (m, 2 H), 1.72–1.61 (m, 1 H), 1.54–1.45 (m, 1 H), 1.36–1.29 (m, 2 H), 0.89 (t, $^3J_{H,H}$ = 8.0 Hz, 3 H) ppm. $^{19}$F NMR ($CDCl_3$): $\delta$ = –74.4 (dq, $^3J_{F-F}$ = 12.3, $^5J_{F-F}$ = 4.9 Hz, 3 F), –74.8 (q, $^4J_{F-F}$ = 9.9 Hz, 3 F), –76.1 (dq, $^4J_{F-F}$ = 9.9, $^5J_{F-F}$ = 4.9 Hz, 3 F), –79.7 (q, $^4J_{F-F}$ = 9.9 Hz, 3 F), –117.2 (dq, $^2J_{F-F}$ = 292.6, $^4J_{F-F}$ = 9.9 Hz, 1 F), –121.5 (dq, $^2J_{F-F}$ = 292.6, $^3J_{F-F}$ = 12.3 Hz, 1 F) ppm. $^{31}$P NMR ($CDCl_3$): $\delta$ = –2.6 ppm. M.p. 84.9–85.7 °C (dec.). $C_{23}H_{17}F_{14}O_2P$ (622.33): calcd. C 44.39, H 2.75; found C 44.48, H 2.75. **12-*endo***: $\delta$ = 7.75 (dd, $^3J_{H-P}$ = 23.2, $^3J_{H,H}$ = 8 Hz, 2 H), 7.67–7.52 (m, 6 H), 2.47–2.38 (m, 2 H), 1.70–1.65 (m, 1 H), 1.52–1.43 (m, 1 H), 1.36–1.24 (m, 2 H), 0.82 (t, $^3J_{H,H}$ = 8.0 Hz, 3 H) ppm. $^{19}$F NMR ($CDCl_3$): $\delta$ = –73.9 (m, 3 F), –74.8 (q, $^4J_{F-F}$ = 9.9 Hz, 3 F), –76.3 (m, 3 F), –80.0 (m, 3 F), –118.0 (d, $^2J_{F-F}$ = 292.0 Hz, 1 F), –121.5 (dq, $^2J_{F-F}$ = 292.0, $^3J_{F-F}$ = 12.3 Hz, 1 F) ppm. $^{31}$P NMR ($CDCl_3$): $\delta$ = –2.8 ppm. M.p. 52.0–53.0 °C (dec.). $C_{23}H_{17}F_{14}O_2P$ (622.33): calcd. C 44.39, H 2.75; found C 44.30, H 2.47.

**12-*exo* from 18-*exo*:** Under $N_2$, *n*BuLi (1.60 M *n*-hexane solution, 0.03 mL, 0.05 mmol) was added to a solution of **18-*exo*** (8.9 mg, 0.016 mmol) in $Et_2O$ (1.5 mL) at 0 °C, which was stirred for 3 h at room temperature. $I_2$ (12 mg, 0.05 mmol) was then added to the

  

mixture at –78 °C which was then stirred for 1 h at room temperature. The reaction was quenched with aqueous $Na_2S_2O_3$ (10 mL). The mixture was extracted with $Et_2O$ (20 mL × 2), and the organic layer was washed with brine (10 mL × 2) and dried with anhydrous $MgSO_4$. After removing the solvents by evaporation, the resulting crude mixture was separated by TLC ($CH_2Cl_2$/*n*-hexane = 1:3) to afford **12-*exo*** (8.6 mg, 0.014 mmol, 87%) as a white solid. The spectroscopic data were consistent with those of the same product described above.

**12-*endo* from 18-*endo*:** Under $N_2$, *n*BuLi (1.60 M *n*-hexane solution, 0.40 mL, 0.64 mmol) was added to a solution of **18-*endo*** (121 mg, 0.214 mmol) in $Et_2O$ (8 mL) at 0 °C and the mixture was stirred for 3 h at room temperature. $I_2$ (162 mg, 0.64 mmol) was then added to the mixture at –78 °C and stirring was continued for 3 h at room temperature. The reaction was quenched with aqueous $Na_2S_2O_3$ (30 mL). The mixture was extracted with $Et_2O$ (50 mL × 2), and the organic layer was washed with brine (30 mL × 2) and dried with anhydrous $MgSO_4$. After removing the solvents by evaporation, the resulting crude mixture was separated by column chromatography (*n*-hexane) to afford **12** (102.8 mg, 0.165 mmol, 77%, **12-*exo*/12-*endo*** = 8:92) as a white solid. The spectroscopic data were consistent with those of the same products described above.

**13-*exo*:** Under $N_2$, DBU (0.014 mL, 0.093 mmol) was added to a solution of **18-*exo*** (25.5 mg, 0.045 mmol) in $CH_3CN$ (2 mL) at room temperature and the mixture was stirred for 1 h. 1-Iodobutane (0.026 mL, 0.23 mmol) was then added to the mixture at room temperature and stirred for 5 h. The mixture was extracted with $Et_2O$ (50 mL × 2), and the organic layer was washed with brine (40 mL × 2) and dried with anhydrous $MgSO_4$. After removing the solvents by evaporation, the resulting crude mixture was separated by column chromatography ($CH_2Cl_2$/*n*-hexane = 2:3) to afford **13-*exo*** (23 mg, 0.037 mmol, 82%) as a white solid. Colorless crystals of **13-*exo*** suitable for X-ray analysis were obtained by recrystallization from $CH_2Cl_2$/*n*-hexane (1:1). $^1$H NMR ($CDCl_3$): $\delta$ = 8.45–8.36 (m, 2 H), 7.75–7.66 (m, 6 H), 2.30–2.16 (m, 2 H), 1.81–1.72 (m, 1 H), 1.61–1.55 (m, 1 H), 1.27 (sextet, $^3J_{H,H}$ = 7.6 Hz, 2 H), 0.80 (t, $^3J_{H,H}$ = 7.6 Hz, 3 H) ppm. $^{19}$F NMR ($CDCl_3$): $\delta$ = –73.4 (dq, $^3J_{F-F}$ = 12.3, $^5J_{F-F}$ = 7.3 Hz, 3 F), –75.1 (q, $^4J_{F-F}$ = 9.8 Hz, 3 F), –75.5 (q, $^4J_{F-F}$ = 9.8 Hz, 3 F), –79.8 (q, $^5J_{F-F}$ = 7.3 Hz, 3 F), –117.5 (d, $^2J_{F-F}$ = 292.0 Hz, 1 F), –119.3 (dq, $^2J_{F-F}$ = 292.0, $^3J_{F-F}$ = 12.3 Hz, 1 F) ppm. $^{31}$P NMR ($CDCl_3$): $\delta$ = –17.2 ppm. M.p. 118.4–119.1 °C. $C_{23}H_{17}F_{14}O_2P$ (622.33): calcd. C 44.39, H 2.75; found C 44.41, H 2.51.

**13-*endo*:** Under $N_2$, to a solution of **18-*endo*** (26 mg, 0.046 mmol) in $CH_3CN$ (2 mL) was added DBU (0.014 mL, 0.093 mmol) at room temperature and the resulting mixture was stirred for 1 h. 1-Iodobutane (0.026 mL, 0.23 mmol) was then added to the mixture at room temperature and stirring was continued for 5 h. The mixture was extracted with $Et_2O$ (50 mL × 2), and the organic layer was washed with brine (50 mL × 2) and dried with anhydrous $MgSO_4$. After removing the solvents by evaporation, the resulting crude mixture was separated by column chromatography ($CH_2Cl_2$/*n*-hexane = 1:1) to afford **13-*endo*** (25 mg, 0.040 mmol, 87%) as a colorless oil. $^1$H NMR ($CDCl_3$): $\delta$ = 8.46–8.40 (m, 2 H), 7.74–7.65 (m, 6 H), 2.30–2.11 (m, 2 H), 1.80–1.71 (m, 1 H), 1.24 (sextet, $^3J_{H,H}$ = 7.2 Hz, 2 H), 1.14–1.08 (m, 1 H), 0.80 (t, $^3J_{H,H}$ = 7.2 Hz, 3 H) ppm. $^{19}$F NMR ($CDCl_3$): $\delta$ = –73.8 (dq, $^3J_{F-F}$ = 9.2, $^5J_{F-F}$ = 6.1 Hz, 3 F), –75.3 (q, $^4J_{F-F}$ = 8.6 Hz, 3 F), –75.4 (q, $^4J_{F-F}$ = 8.6 Hz, 3 F), –79.4 (q, $^5J_{F-F}$ = 6.1 Hz, 3 F), –118.0 (dq, $^2J_{F-F}$ = 289.6, $^4J_{F-F}$ = 9.9 Hz, 3 F), –119.2 (dq, $^2J_{F-F}$ = 289.6, $^3J_{F-F}$ = 9.2 Hz, 3 F) ppm. $^{31}$P NMR ($CDCl_3$): $\delta$ = –17.6 ppm. $C_{23}H_{17}F_{14}O_2P$ (622.33): calcd. C 44.39, H 2.75; found C 44.14, H 2.39.

**Single Crystal X-ray Analysis of 12-*exo*, 13-*exo*, 18-*exo*, and 18-*endo*:** Crystals suitable for X-ray structural determination were mounted on a Mac Science DIP2030 imaging plate diffractometer and irradiated with graphite-monochromated Mo-$K_\alpha$ radiation ($\lambda$ = 0.71073 Å). The unit cell parameters were determined by separately autoindexing several images in each data set using the DENZO program (MAC Science).[33] For each data set, the rotation images were collected in 3° increments with a total rotation of 180° about

Table 6. Crystallographic data for **18-*exo***, **18-*endo***, **12-*exo***, and **13-*exo***.

| Compound | **18-*exo*** | **18-*endo*** | **12-*exo*** | **13-*exo*** |
|---|---|---|---|---|
| Formula | $C_{19}H_9F_{14}O_2P$ | $C_{19}H_9F_{14}O_2P$ | $C_{23}H_{17}F_{14}O_2P$ | $C_{23}H_{17}F_{14}O_2P$ |
| Molecular weight | 566.22 | 566.22 | 622.33 | 622.33 |
| Crystal system | monoclinic | monoclinic | monoclinic | orthorhombic |
| Space group | $P2_1/n$ | $P2_1/c$ | $P2_1/a$ | $Pbca$ |
| Color | colorless | colorless | colorless | colorless |
| Habit | plate | plate | plate | plate |
| Crystal dimensions [mm] | 0.50 × 0.40 × 0.35 | 0.60 × 0.35 × 0.30 | 0.50 × 0.35 × 0.35 | 0.60 × 0.25 × 0.25 |
| $a$ [Å] | 11.8640(3) | 11.6690(11) | 14.7780(2) | 11.8430(5) |
| $b$ [Å] | 11.6400(3) | 15.4580(11) | 9.2830(2) | 25.6240(9) |
| $c$ [Å] | 15.1210(3) | 11.9110(10) | 19.9340(4) | 16.6250(2) |
| $\alpha$ [°] | 90 | 90 | 90 | 90 |
| $\beta$ [°] | 96.6630(10) | 111.616(4) | 110.8040(10) | 90 |
| $\gamma$ [°] | 90 | 90 | 90 | 90 |
| $V$ [Å$^3$] | 2074.06(3) | 1997.4(3) | 2556.33(8) | 5045.1(3) |
| $Z$ | 4 | 4 | 4 | 8 |
| $D_{calcd.}$ [g cm$^{-3}$] | 1.813 | 1.883 | 1.617 | 1.639 |
| Absorption coefficient [mm$^{-1}$] | 0.274 | 0.284 | 0.230 | 0.233 |
| $F$(000) | 1120 | 1120 | 1248 | 2496 |
| Radiation, $\lambda$ [Å] | Mo-$K_\alpha$, 0.71073 | Mo-$K_\alpha$, 0.71073 | Mo-$K_\alpha$, 0.71073 | Mo-$K_\alpha$, 0.71073 |
| $T$ [K] | 298 | 130 | 298 | 298 |
| Data collected | $+h$, $+k$, $\pm l$ | $+h$, $+k$, $\pm l$ | $+h$, $+k$, $\pm l$ | $+h$, $+k$, $+l$ |
| Data / restraints / parameters | 4972 / 0/329 | 2930 / 0/325 | 6113 / 0 / 362 | 5548 / 0 / 362 |
| $R_1$ [$I > 2\sigma(I)$] | 0.0684 | 0.0626 | 0.0731 | 0.0844 |
| $wR_2$ (all data) | 0.2003 | 0.1717 | 0.2372 | 0.2683 |
| GOF | 1.091 | 1.132 | 1.088 | 1.115 |
| Solvent for crystallization | $CH_3CN$ | $Et_2O$/*n*-hexane | *n*-hexane | *n*-hexane/$CH_2Cl_2$ |

  

the ϕ axis. The data were processed by using SCALEPACK. The structure was solved by a direct method using the SHELX-97 program.[34] Refinement on $F^2$ was carried out by full-matrix least-squares by using the SHELX-97 program.[34] All non-hydrogen atoms were refined by using anisotropic thermal parameters. The hydrogen atoms were included in the refinement with isotropic thermal parameters. The crystallographic data are summarized in Table 6.

CCDC-652187 (for **12-*exo***), -652188 (for **13-*exo***), -652189 (for **18-*exo***) and -652190 (for **18-*endo***) contain the supplementary crystallographic data for this paper. These data can be obtained free of charge from the Cambridge Crystallographic Data Centre via www.ccdc.cam.ac.uk/data_request/cif.

**Kinetic Measurements for the Stereomutation Between 13-*exo* and 13-*endo*:** Samples (ca. 10 mg) of **13-*exo*** dissolved in freshly distilled 4-*tert*-butyltoluene were sealed in NMR tubes under $N_2$. Kinetic measurements of the pseudorotation process was carried out using a JEOL EX-400 spectrometer by monitoring the change in the diastereomeric ratio (**13-*exo*/13-*endo***) from the integral values of the $^{19}F$ NMR signals. The measurements were recorded in the temperature range of 190–210 °C. The data were analyzed assuming reversible first-order kinetics using the equation $\ln[(C_e - C_0)/(C_e - C)] = k_{-}(K+1)t$, where $C_e$ is the equilibrium ratio, $C_0$ the ratio observed at $t = 0$, $C$ the ratio observed at fixed intervals, $K$ the equilibrium constant [$K = (100 - C_e)/C_e = k_+/k_-$], $k_+$ = the rate constant for the stereomutation of **13-*exo*** to **13-*endo***, and $k_-$ is the rate constant for the stereomutation of **13-*endo*** to **13-*exo***.[35] The rate constants and calculated activation parameters for the stereomutation are shown in Table 4.

**Kinetic Measurements for the Pseudorotation of 12-*exo* or 12-*endo* to 13:** Samples (ca. 10 mg) of **12-*exo*** or **12-*endo*** dissolved in 4-*tert*-butyltoluene (0.6 mL) were sealed in a NMR tube under $N_2$. Kinetic measurements of the pseudorotation process were carried out on a JEOL EX-400 spectrometer by monitoring the $^{19}F$ NMR signals in a variable-temperature mode, and the specified temperatures were maintained throughout each set of measurements (error within ±1 °C). The observed temperatures were calibrated by using the $^1H$ NMR chemical shift differences of the signals of neat 1,3-propanediol (high-temperature region) and MeOH (low-temperature region).

The data for the conversion of **12-*exo*** to **13** were analyzed assuming first-order kinetics by using Equations (1) and (2), where $C_0$ is the ratio of **12-*exo*** observed at $t = 0$, $C_{12\text{-}exo}$ the ratio of **12-*exo*** observed at constant intervals, $C_{13\text{-}exo}$ the ratio of **13-*exo*** observed at constant intervals, $C_{13\text{-}endo}$ the ratio of **13-*endo*** observed at constant intervals, $k_{exo}$ the rate constant for the pseudorotation of **12-*exo*** to **13-*exo***), and $k_{endo}$ is the rate constant for the pseudorotation of **12-*exo*** to **13-*endo***.[35] The ratios of $C_0/C_{12\text{-}exo}$ and $C_{13\text{-}endo}/C_{13\text{-}exo}$ were monitored by $^{19}F$ NMR at 40, 45, 50, 55, and 60 °C. The stereomutation of **12-*endo*** to **13** was also analyzed by the same method. The rate constants and activation parameters for the stereomutation of **12** to **13** are summarized in Table 5.

$$\ln(C_0/C_{12\text{-}exo}) = (k_{exo} + k_{endo})t \quad (1)$$

$$k_{endo}/k_{exo} = C_{13\text{-}endo}/C_{13\text{-}exo} \quad (2)$$

## Acknowledgments

The authors are grateful to Central Glass Co., Ltd., for the generous gift of hexafluorocumyl alcohol. This work was supported by two Grants-in-Aid for Scientific Research on Priority Areas from the Ministry of Education, Culture, Sports, Science and Technology (MEXT) (Project Nos. 14340199 and 17350021) .

[1] a) K.-y. Akiba, *Chemistry of Hypervalent Compounds*, Wiley-VCH, New York, **1999**; b) R. R. Homes, *Pentacoordinated Phosphorus – Structure and Spectroscopy*; ACS Monographs 175 and 176, vol. I and II, American Chemical Society, Washington, DC, **1980**; c) D. E. C. Corbridge, *Phosphorus: An Outline of Its Chemistry, Biochemistry and Technology*, 4th ed.; Elsevier, Amsterdam, **1990**, chapter 14, pp. 1233–1256; d) R. Burgada, R. Setton in *The Chemistry of Organophosphorus Compounds* (Ed.: F. R. Hartley), Wiley-Interscience, Chichester, **1994**, vol. 3, pp. 185–277.

[2] For the *N*-X-*L* designation, see: C. W. Perkins, J. C. Martin, A. J. Arduengo, W. Lau, A. Alegria, J. K. Kochi, *J. Am. Chem. Soc.* **1980**, *102*, 7753–7759.

[3] a) A. C. Hengge, *Acc. Chem. Res.* **2002**, *35*, 105–112, and references cited therein; b) S. D. Lahiri, G. Zhang, D. Dunaway-Mariano, K. N. Allen, *Science* **2003**, *299*, 2067–2071; c) R. R. Holmes, *Acc. Chem. Res.* **2004**, *37*, 746–753; d) F. H. Westheimer, *Acc. Chem. Res.* **1968**, *1*, 70–78; e) G. R. J. Thatcher, R. Kluger, *Adv. Phys. Org. Chem.* **1989**, *25*, 99–265; for recent mechanistic studies on phosphoryl transfer reactions; see: f) C. S. López, O. N. Faza, A. R. de Lera, D. M. York, *Chem. Eur. J.* **2005**, *11*, 2081–2093, and references cited therein; g) T. Uchimaru, M. Uebayasi, T. Hirose, S. Tsuzuki, A. Yliniemelä, K. Tanabe, K. Taira, *J. Org. Chem.* **1996**, *61*, 1599–1608.

[4] a) W. S. Wadsworth Jr, *Org. React.* **1977**, *25*, 73–253; b) J. I. G. Cadogan, *Organophosphorus Reagents in Organic Synthesis*, Academic Press, New York, **1979**; c) B. E. Maryanoff, A. B. Reitz, *Chem. Rev.* **1989**, *89*, 863–927; d) S. E. Kelly in *Comprehensive Organic Synthesis* (Eds.: B. M. Trost, I. Fleming); Pergamon Press, Oxford, **1991**,vol. 1, pp. 730–817; e) A. W. Johnson, *Ylides and Imines of Phosphorus*, Wiley-Interscience, New York, **1993**; f) E. Vedejs, M. J. Peterson, *Top. Stereochem.* **1994**, *21*, 1–157; g) E. Vedejs, M. J. Peterson, *Adv. Carbanion Chem.* **1996**, *2*, 1–85.

[5] a) M. Nakamoto, S. Kojima, S. Matsukawa, Y. Yamamoto, K.-y. Akiba, *J. Organomet. Chem.* **2002**, *643–644*, 441–452; b) S. Matsukawa, K. Kajiyama, S. Kojima, S.-y. Furuta, Y. Yamamoto, K.-y. Akiba, *Angew. Chem. Int. Ed.* **2002**, *41*, 4718–4722; c) S. Trippett, *Phosphorus Sulfur* **1976**, *1*, 89–98; d) S. Trippett, *Pure Appl. Chem.* **1974**, *40*, 595–604; e) G. Buono, J. R. Llinas, *J. Am. Chem. Soc.* **1981**, *103*, 4532–4540; f) M. Eisenhut, H. L. Mitchell, D. D. Traficante, R. J. Kaufman, J. M. Deutsch, G. M. Whitesides, *J. Am. Chem. Soc.* **1974**, *96*, 5385–5397; g) C. G. Moreland, G. O. Doak, L. B. Littlefield, N. S. Walker, J. W. Gilje, R. W. Braun, A. H. Cowley, *J. Am. Chem. Soc.* **1976**, *98*, 2161–2165; h) L. V. Griend, R. G. Cavell, *Inorg. Chem.* **1983**, *22*, 1817–1820; i) S. Kumaraswamy, C. Muthiah, K. C. Kumara Swamy, *J. Am. Chem. Soc.* **2000**, *122*, 964–965; j) P. Kommana, S. Kumaraswamy, J. J. Vittal, K. C. Kumara Swamy, *Inorg. Chem.* **2002**, *41*, 2356–2363; k) P. Kommana, N. S. Kumar, J. J. Vittal, E. G. Jayasree, E. D. Jemmis, K. C. Kumara Swamy, *Org. Lett.* **2004**, *6*, 145–148.

[6] a) R. Hoffmann, J. M. Howell, E. L. Muetterties, *J. Am. Chem. Soc.* **1972**, *94*, 3047–3058; b) R. S. McDowell, A. Streitwieser Jr, *J. Am. Chem. Soc.* **1985**, *107*, 5849–5855; c) J. A. Deiters, R. R. Holmes, J. M. Holmes, *J. Am. Chem. Soc.* **1988**, *110*, 7672–7681; d) P. Wang, Y. Zhang, R. Glaser, A. E. Reed, P. v. R. Schleyer, A. Streitwieser Jr, *J. Am. Chem. Soc.* **1991**, *113*, 55–64; e) H. Wasada, K. Hirao, *J. Am. Chem. Soc.* **1992**, *114*, 16–27; f) G. R. J. Thatcher, A. S. Campbell, *J. Org. Chem.* **1993**, *58*, 2272–2281; g) P. Wang, Y. Zhang, R. Glaser, A. Streitwieser, P. v. R. Schleyer, *J. Comput. Chem.* **1993**, *14*, 522–529; h) B. D. Wladkowski, M. Krauss, W. J. Stevens, *J. Phys. Chem.* **1995**, *99*, 4490–4500.

[7] a) R. S. Berry, *J. Chem. Phys.* **1960**, *32*, 933–938; b) K. Mislow, *Acc. Chem. Res.* **1970**, *3*, 321–331; c) E. L. Muetterties, *Acc.*

  

*Chem. Res.* **1970**, *3*, 266–273; d) I. Ugi, D. Marquarding, H. Klusacek, P. Gillespie, F. Ramirez, *Acc. Chem. Res.* **1971**, *4*, 288–296; e) P. Gillespie, P. Hoffman, H. Klusacek, D. Marquarding, S. Pfohl, F. Ramirez, E. A. Tsolis, I. Ugi, *Angew. Chem. Int. Ed. Engl.* **1971**, *10*, 687–715.

[8] J. Moc, K. Morokuma, *J. Am. Chem. Soc.* **1995**, *117*, 11790–11797.

[9] a) J. A. Altmann, K. Yates, I. G. Csizmadia, *J. Am. Chem. Soc.* **1976**, *98*, 1450–1454; b) A. Strich, A. Veillard, *J. Am. Chem. Soc.* **1973**, *95*, 5574–5581; c) S.-K. Shih, S. D. Peyerimhoff, *J. Chem. Soc. Faraday Trans. 2.* **1979**, *75*, 379–389.

[10] J. C. Martin, *Science* **1983**, *221*, 509–514.

[11] a) S. Kojima, K. Kajiyama, M. Nakamoto, K.-y. Akiba, *J. Am. Chem. Soc.* **1996**, *118*, 12866–12867; b) K. Kajiyama, M. Yoshimune, M. Nakamoto, S. Matsukawa, S. Kojima, K.-y. Akiba, *Org. Lett.* **2001**, *3*, 1873–1875; c) S. Kojima, K. Kajiyama, M. Nakamoto, S. Matsukawa, K.-y. Akiba, *Eur. J. Org. Chem.* **2006**, 218–234; d) K. Kajiyama, M. Yoshimune, S. Kojima, K.-y. Akiba, *Eur. J. Org. Chem.* **2006**, 2739–2746.

[12] Some compounds that violate the apicophilicity concept have been isolated. In these cases, some sort of steric constraints disallowed regular configurations: a) J. Kobayashi, K. Goto, T. Kawashima, *J. Am. Chem. Soc.* **2001**, *123*, 3387–3388; b) J. Kobayashi, K. Goto, T. Kawashima, M. W. Schmidt, S. Nagase, *J. Am. Chem. Soc.* **2002**, *124*, 3703–3712; c) S. Vollbrecht, A. Vollbrecht, J. Jeske, P. G. Jones, R. Schmutzler, W.-W. du Mont, *Chem. Ber./Recueil* **1997**, *130*, 819–822.

[13] By introducing a very bulky bidentate ligand, some of the phosphoranes become thermodynamically stable species even though the regular configurations are allowed: a) K. C. Kumara Swamy, N. S. Kumar, *Acc. Chem. Res.* **2006**, *39*, 324–333; b) K. V. P. P. Kumar, N. S. Kumar, K. C. Kumara Swamy, *New J. Chem.* **2006**, *30*, 717–728; c) A. Chandrasekaran, N. V. Timosheva, R. R. Holmes, *Phosphorus Sulfur Silicon Relat. Elem.* **2006**, *181*, 1493–1511; d) N. S. Kumar, P. Kommana, J. J. Vittal, K. C. Kumara Swamy, *J. Org. Chem.* **2002**, *67*, 6653–6658.

[14] S. Matsukawa, S. Kojima, K. Kajiyama, Y. Yamamoto, K.-y. Akiba, S. Re, S. Nagase, *J. Am. Chem. Soc.* **2002**, *124*, 13154–13170.

[15] T. Adachi, S. Matsukawa, M. Nakamoto, K. Kajiyama, S. Kojima, Y. Yamamoto, K.-y. Akiba, S. Re, S. Nagase, *Inorg. Chem.* **2006**, *45*, 7269–7277.

[16] S. Kojima, M. Sugino, M. Nakamoto, S. Matsukawa, K.-y. Akiba, *J. Am. Chem. Soc.* **2002**, *124*, 7674–7675.

[17] For the proposed nomenclature system of the optically active pentacoordinate molecules, see: J. C. Martin, T. M. Balthazor, *J. Am. Chem. Soc.* **1977**, *99*, 152–162.

[18] S. Kojima, M. Nakamoto, K.-y. Akiba, submitted.

[19] a) P. R. Wells, *Prog. Phys. Org. Chem.* **1968**, *6*, 111–145; b) N. Inamoto, S. Masuda, *Chem. Lett.* **1982**, 1003–1006; c) J. Mullay, *J. Am. Chem. Soc.* **1985**, *107*, 7271–7275, and references cited therein; d) D. Bergmann, J. Hinze, *Angew. Chem. Int. Ed. Engl.* **1996**, *35*, 150–163, and references cited therein; e) C. H. Suresh, N. Koga, *J. Am. Chem. Soc.* **2002**, *124*, 1790–1797.

[20] X.-D. Jiang, K.-i. Kakuda, S. Matsukawa, H. Yamamichi, S. Kojima, Y. Yamamoto, *Chem. Asian J.* **2007**, *2*, 314–323.

[21] a) H. B. Powell, J. J. Lagowski, *J. Chem. Soc.* **1962**, 2047–2049; b) H. B. Powell, J. J. Lagowski, *J. Chem. Soc.* **1965**, 1392–1396; c) G. V. D. Tiers, *J. Am. Chem. Soc.* **1956**, *78*, 2914–2915; d) C.-H. Deng, C.-J. Guan, M.-H. Shen, C.-X. Zhao, *J. Fluorine Chem.* **2002**, *116*, 109–115.

[22] A. Kruse, I. Ruppert, US Pat. 5017719 [*Chem. Abstr.* **1989**, *111*, 77646].

[23] a) R. P. Singh, G. Cao, R. L. Kirchmeier, J. M. Shreeve, *J. Org. Chem.* **1999**, *64*, 2873–2876; b) R. P. Singh, J. M. Shreeve, *Tetrahedron* **2000**, *56*, 7613–7632; c) G. K. S. Prakash, A. K. Yudin, *Chem. Rev.* **1997**, *97*, 757–786.

[24] E. F. Perozzi, R. S. Michalak, G. D. Figuly, W. H. Stevenson III, D. B. Dess, M. R. Ross, J. C. Martin, *J. Org. Chem.* **1981**, *46*, 1049–1053.

[25] S. K. Chopra, J. C. Martin, *Heteroat. Chem.* **1991**, *2*, 71–79.

[26] N. Lozac'h in *Comprehensive Heterocyclic Chemistry* (Eds.: A. R. Katritzky, C. W. Rees), Pergamon Press, Oxford, **1984**, vol. 6, pp. 1049–1070.

[27] a) P. Livant, J. C. Martin, *J. Am. Chem. Soc.* **1977**, *99*, 5761–5767; b) L. J. Adzima, E. N. Duesler, J. C. Martin, *J. Org. Chem.* **1977**, *42*, 4001–4005; c) W. Y. Lam, E. N. Duesler, J. C. Martin, *J. Am. Chem. Soc.* **1981**, *103*, 127–135.

[28] S. Kojima, M. Nakata, K. Kajiyama, K.-y. Akiba, *Tetrahedron Lett.* **1997**, *38*, 2261–2265.

[29] The term "pivot" means one of the three equatorial substituents which remains at the equatorial site during the Berry psudorotation process. For more details, see ref.[7b,7d,7e].

[30] For example: S. Kojima, M. Nakata, K. Yamazaki, K.-y. Akiba, *Tetrahedron Lett.* **1997**, *38*, 4107–4110.

[31] X.-D. Jiang, S. Matsukawa, H. Yamamichi, Y. Yamamoto, *Heterocycles*, **2007**, *73*, in press.

[32] E. L. Eliel, S. H. Wilen, L. N. Mander, *Stereochemistry of Organic Compounds*, Wiley Interscience, New York, **1994**.

[33] Z. Otwinowski, W. Minor, *Methods in Enzymology*, vol. 276: *Macromolecular Crystallography*, Part A (Eds.: C. W. Carter Jr, R. M. Sweet), Academic Press, **1997**, pp. 307–326.

[34] G. M. Sheldrick, *SHELX-97*, University of Göttingen, Göttingen, **1997**.

[35] J. H. Espenson, *Chemical Kinetics and Reaction Mechanisms*, 2nd ed., McGraw-Hill, New York, **1995**.

Received: October 16, 2007
Published Online: January 11, 2008

  